Effect of the degree of acetylation on the physicochemical properties of α-chitin nanofibers

Junnosuke MACHIDA[a], Shin SUENAGA[a], and Mitsumasa OSADA[a,*]

[a]Department of Chemistry and Materials, Faculty of Textile Science and Technology, Shinshu University, 3-15-1, Tokida, Ueda, Nagano 386-8567, Japan

*Corresponding author. Tel.: +81-268-21-5458; Fax: +81-268-21-5391

E-mail: osadam@shinshu-u.ac.jp

1. Introduction

Chitin, a long-chain polysaccharide consisting of β-(1,4)-linked *N*-acetyl anhydroglucosamine units, is the second most abundant biopolymer on Earth after cellulose [1]. Chitin has a hierarchical structure based on chitin nanofibers (ChNFs), which has attracted research interest in materials engineering [2–4]. Although chitin powder is insoluble in water, ChNFs can be dispersed homogeneously in water, which makes them easy to handle and shape into desired forms [5–7]. There are two types of chitin, namely, α-chitin and β-chitin, which have different crystalline structures [8,9]. β-Chitin consists of parallel molecular chains without significant hydrogen bonding between intermolecular sheets [10–12]; therefore, β-chitin powder can be easily disintegrated into nanofibers (NFs) [13,14]. In contrast, α-chitin consists of antiparallel molecular chains with hydrogen bonds between the chains [8], which makes it difficult to disintegrate α-chitin powder into NFs [15]. As a result, the physicochemical properties, such as transmittance and viscosity, of α-ChNF dispersions cannot be varied as widely as those of β-ChNF dispersions [16,17]. However, α-chitin, which is obtained industrially from the exoskeletons of crustaceans, has a higher natural abundance than β-chitin [18,19]. Therefore, to utilize α-chitin effectively, it is necessary to realize control of the physicochemical properties α-ChNF dispersions, as is possible for β-ChNF dispersions. For example, studies on β-ChNFs have shown that thin NFs with narrow distributions provide dispersions with high transmittances and high viscosities [16].

To control the physicochemical properties of α-ChNF dispersions, it is necessary to weaken the strong hydrogen bonds between the chitin molecular chains. It has been reported that the deacetylation of chitin by alkaline treatment can weaken the interchain hydrogen bonding interactions. In nature, 95% of the groups at the C-2 position of α-chitin are acetoamide groups with the other 5% being amino groups; this corresponds to a degree of

acetylation (DA) of 95%. Fan et al. prepared partially deacetylated chitin, with a DA of 70–74%, by alkaline treatment [20]. Thereafter, the amine groups were cationized by adding acid. Owing to electrostatic repulsion between the molecular chains of the cationized chitin, disintegration of the α-chitin powder into NFs proceeded easily by sonication for 1 min. However, as the range of reported DAs (70–74%) is limited, the effect of DA on the physicochemical properties of α-ChNFs has not been clearly established.

In addition, it is difficult to establish the exact effect of deacetylation on the properties of ChNFs because it is difficult to control the concentration of insoluble ChNFs in water. As chitin powder consists of NF bundles, deacetylation proceeds from the surface of the NFs. Therefore, the deacetylated part, namely, the part containing amino groups, is dissolved by acid treatment. In this case, at a fixed amount of loaded chitin, the net amount of ChNFs is affected by dissolution. However, the physicochemical properties of ChNFs are dependent on the number of dispersed NFs, not dissolved NFs. Therefore, in this work, α-chitin with different DAs was prepared by varying the deacetylation treatment time. Then, to determine the exact amount of ChNFs, we weighed the solid residues after acid treatment and then prepared dispersions of the ChNFs with different DAs at a constant concentration to evaluate the physicochemical properties. Furthermore, as the width and the distribution of NFs affect transmittance and viscosity, a simple method for estimating the average NF width at different DAs was suggested.

2. Materials and methods

2.1 Materials and preparation of ChNFs

α-Chitin powder with a DA of 95% and particle sizes of ≤100 μm was purchased from Nacalai Tesque Inc. (Kyoto, Japan). The preparation of ChNFs at different DAs was conducted as summarized in Fig. 1. α-Chitin powder (4 wt%) was suspended in 12 mol/L

NaOH aqueous solution and deacetylated for 6–340 h at 70°C. After the deacetylation treatment, the sample was centrifuged (MX-305, Tomy Seiko Co., Ltd., Tokyo, Japan) at 7,500 × *g* at room temperature for 5 min and the supernatant was removed. The obtained deacetylated chitin powder was washed using centrifugation at 7,500 × *g* for 5 min and decantation using distilled water. The partially deacetylated chitin was mixed with 0.1 mol/L acetic acid aqueous solution and then separated into soluble and insoluble parts using centrifugation at 7,500 × *g* for 5 min.

In the presence of acetic acid, the amino groups in chitin are protonated, resulting in electrostatic repulsion between the NFs. Therefore, we believe that the ratio between the amino groups in chitin and acetic acid is important. In accordance with a previous study [16], we have defined the acidity as follows:

$$\text{Acidity [mol/mol]} = \text{amount of acetic acid [mol]} / \text{number of amino groups in chitin [mol]} \quad (1)$$

In this work, all experiments were conducted at an acidity of 0.9. We previously studied the effect of acidity on the physicochemical properties of α-chitin nanofiber dispersions [16]. In that work, we confirmed that transmittance and viscosity increased with acidity until a value of 0.9, and these factors did not change largely above 0.9. Therefore, we chose an acidity of 0.9 in this study.

We evaluated the weight change of chitin after the acetic acid treatment as follows:

$$\text{Weight change [\%]} = \text{weight of insoluble chitin after acetic acid treatment [g]} / \text{weight of chitin before acetic acid treatment [g]} \times 100. \quad (2)$$

The acetic-acid-insoluble part, namely, the solid residue, was weighed and then used as deacetylated chitin to prepare ChNF dispersions. After suspension of the deacetylated chitin (1 wt%) in distilled water, disintegration into NFs was performed using a Star Burst system (Star Burst Mini, Sugino Machine Co., Ltd., Uozu, Japan). The solid residue can be

converted to nanofibers completely by the Star Burst system, and the details of the disintegration process was described in our previous report [16]. In brief, the suspension was pressurized at approximately 75 MPa and the number of collisions with the ceramic ball was set between 1 and 10 (i.e., 1–10 passes). For chitin with a DA of 95%, namely, unmodified chitin, the pressure was set at 235 MPa because disintegration into NFs did not proceed at 75 MPa.

2.2 Elemental analysis for DA evaluation

To evaluate the DA, the amounts of nitrogen and carbon in unmodified and deacetylated chitin were measured using an elemental analyzer (SUMIGRAPH NC-1000, Sumika Chemical Analysis Service, Ltd., Osaka, Japan). Acetanilide was used as a reference material. Chitin consists of *N*-acetyl glucosamine units, which have a carbon/nitrogen ratio of 8:1, and glucosamine units, which have a carbon/nitrogen ratio of is 6:1. Therefore, the DA was calculated using the following equation:

$$\mathrm{DA} = (C/N - 6)/2 \times 100, \quad (3)$$

where C is the moles of carbon and N is the moles of nitrogen. For the *N*-acetyl glucosamine unit, which has a C/N of 8, the DA is 100%, as calculated by eq. (3). For the glucosamine unit, which has a C/N of 6, the DA is 0%. The DA was determined using the deacetylated chitin powder and solid residue, as shown in Fig. 1.

2.3 Field-emission scanning electron microscopy (FE-SEM)

To prepare the FE-SEM samples, the dispersion of ChNFs in water was diluted with *tert*-butyl alcohol and then precipitated by centrifugation at 20,000 × *g* at room temperature for 5 min. After repeating this process several times, the supernatant was changed from water to *tert*-butyl alcohol. The precipitated sample was frozen in a glass bottle and dried under vacuum conditions (0.02 MPa) for a few hours. The dried and deacetylated ChNFs were coated with an osmium layer (~2 nm thick) using an osmium coater (Neoc-STP, Meiwafosis

Co., Ltd., Tokyo, Japan). The sample was observed using a field-emission scanning electron microscope (S-5000, Hitachi Co., Ltd., Tokyo, Japan) operated at 5.0 kV. A histogram of the ChNF widths was constructed from several FE-SEM images using the Image-J software (NIH, Bethesda, MD, USA).

2.4 Fourier transform infrared (FT-IR) spectroscopy

The deacetylated chitin powders were blended with potassium chloride and converted into pellets using a mini hand-press machine (MHP-1, Shimadzu Co., Ltd., Kyoto, Japan). FT-IR spectra of the pellets were recorded using an FT-IR spectrometer (FT/IR 4200, Jasco Co., Ltd., Tokyo, Japan) from 500 to 4000 cm^{-1}, with 4 cm^{-1} resolution and 32 scans.

To evaluate the DA, FT-IR spectra of unmodified and deacetylated chitin powders (not blended with potassium chloride) were measured using an FT-IR spectrometer (IRPrestige21, Shimadzu Co., Ltd., Kyoto, Japan) equipped with an attenuated total reflection (ATR) unit (DuraSamplIR II, Smiths Detection Inc., London, UK) from 600 to 4000 cm^{-1}, with 4 cm^{-1} resolution and 40 scans. The DA was calculated by using the following equation [21]:

$$DA = (A1320/A1420 - 0.3822)/0.03133 \times 100, \quad (4)$$

where $A1320$ and $A1420$ are the absorbance values measured at 1320 and 1420 cm^{-1}, which correspond to the stretching and bending vibrations of amide III and CH_2 groups, respectively. Their magnitudes were determined via the baseline method proposed in a previous study [21].

2.5 Optical transmittance

The ChNF dispersions (1 wt%) were loaded into quartz cuvettes. The transmittance was measured in the range 200–700 nm at 25°C using a spectrophotometer (V530, Jasco Co., Ltd., Tokyo, Japan) with distilled water as the blank. The transmittance at 600 nm was used to compare different conditions.

2.6 Viscoelastic measurements

The ChNF dispersions were loaded into 50 mL glass bottles. After stirring at 2000 rpm for 1 min, the samples were defoamed at 2000 rpm for 1 min using a mixer (ARE-250, Thinky Co., Ltd., Tokyo, Japan). The deformed ChNF dispersions were placed in a thermostat chamber filled with water at 25 °C, and the viscosity was measured with a Brookfield viscometer (DV-1 Prime, Brookfield Engineering Laboratories Inc., Middleboro, MA, USA). A #64 spindle was used at viscosities above 1000 mPa s, whereas a #62 spindle was used at viscosities below 1000 mPa s. First, the rotating speed was increased to 30, 50, and 100 rpm, and the viscosity at 600 s was used to compare the different conditions. Then, the rotating speed was decreased to 50 and 30 rpm, and the viscosity at 300 s was used to compare the different conditions.

3. Results

3.1 Deacetylation of chitin powder

We compared the DA values obtained by the elemental analysis and FT-IR spectroscopy (Fig. S1). For the untreated chitin powder, the DA obtained by the the elemental analysis was 95% by and that obtained by the FT-IR spectroscopy was 94%. For the deacetylated chitin powder after 18 h of the NaOH aqueous solution treatment, the DA was 59% (elemental analysis) and 60% (FT-IR spectroscopy). Therefore, these results indicate that the DA is accurate. The DA obtained by the elemental analysis will be shown hereafter.

Fig. 2 shows the relationship between the NaOH aqueous solution treatment time and the DA of the deacetylated chitin powder and solid residue shown in Fig. 1. Over the first 6 h, the DA of the deacetylated chitin powder decreased quickly from 95% to 70% and then decreased more gradually, reaching 10% after 270 h. The change in the deacetylation reaction rate observed at ~70% probably occurred because deacetylation proceeds gradually from the

surface to the interior of the ChNFs, as will be discussed later. The DA of the solid residue are higher than that of the deacetylated chitin powder, which was probably due to the elimination of deacetylated surfaces by the acid treatment, as will be discussed later. Hereafter, we consider the results obtained by using the DA value of the deacetylated chitin powder.

Fig. 3 shows the weight change of the deacetylated chitin powder after the acetic acid treatment. The weight of the chitin powder decreased with the decrease in DA, reaching 56% at a DA of 35%. As the deacetylated part of the chitin powder was dissolved in acetic acid, the amount dissolved in acetic acid increased with decreasing DA.

The effects of DA on the FT-IR spectra of the deacetylated chitin powder are shown in Fig. 4. The peak at 3300 cm^{-1} is derived from N–H stretching, the peaks at 1655 and 1630 cm^{-1} are amide I bands, and the peak at 1550 cm^{-1} is an amide II band [21]. The transmittances of these peaks decreased with decreasing DA, probably because of the change from –NH–$COCH_3$ to –NH_2 at C-2 in chitin with decreasing DA [22,23].

3.2 Effect of DA on ChNF width

FE-SEM images and the width distributions of the ChNFs at different DAs are shown in Figs. 5–7. At a DA of 95% (Fig. 5), the average and standard deviation of the ChNF width after 10 passes were 34 nm and 24 nm, respectively. The ChNF widths within 10 passes were greater (data not shown). In our previous study, an increased pass time resulted in decreased ChNF widths because of an increase in the kinetic energies imparted to the NF bundles [16,24].

At a DA of 66% (Fig. 6), the average ChNF widths after 1 and 2 passes were similar (~30 nm); however, the average width decreased to 18 nm after 10 passes. At a DA of 35% (Fig. 7), the average width was only 20 nm after 1 pass, and it decreased slightly to ~18 nm after 2 and 10 passes. This result indicates that at lower DAs, it becomes easier to form thin

NFs from chitin, and a decrease in the NF width can be achieved within a few passes.

3.3 Effect of DA on the transmittance of ChNF dispersions

The effect of DA on the transmittance of the ChNF dispersions is shown in Fig. 8. At a DA of 95%, the transmittance was 0%, even after 10 passes. At a DA of 66%, the transmittance was 0% after 1 and 2 passes; however, it increased to 18% after 5 passes and 49% after 10 passes. At a DA of 52%, even 1 and 2 passes increased the transmittance, with the transmittance reaching 31% after 5 passes and 56% after 10 passes. At a DA of 46%, the transmittance was 29% after 1 pass and it reached 67% after 10 passes. At a DA of 35%, the transmittance reached 57% after 1 pass and 67% after 10 passes. At a DA of 20%, the transmittance was not greatly affected by the number of passes (64% and 69% after 1 pass and 10 passes, respectively). From these results, as the DA decreased, few passes were required to increase the transmittance of the ChNF dispersions.

From our previous research, the transmittance of ChNF dispersions increased with decreasing NF width, even at a DA of 95% [16]. NFs with a narrow width distribution resulted in high transmittance because the homogeneous structure inhibits multiple scattering. In this work, at lower DAs, the NF width could be decreased with fewer passes, as shown by the FE-SEM observations in Fig. 5–7. Therefore, the increase in transmittance with decreasing NF width was controlled by the DA.

Interestingly, the maximum transmittance was ~70%, regardless of the DA or number of passes. As shown in Fig. 7 for a DA of 35%, the average NF width was maintained at ~17 nm, even after 10 passes. Because the NF width could not be decreased to less than 17 nm and the network structure of the NFs was not changed after 10 passes, a transmittance higher than 70% could not be obtained.

3.4 Effect of DA on the viscosity of ChNF dispersions

The effect of the DA on the viscosities of the ChNFs dispersions is shown in Fig. 9.

At a DA of 95%, the viscosity was 110 mPa s, even after 10 passes. At a DA of 66%, the viscosity increased after 1 and 2 passes, reaching 1300 mPa s after 3 passes and 1200 mPa s after 5 passes. At a DA of 52%, the viscosity increased after 1 and 2 passes to reach 2500 mPa s and then decreased after 5 and 10 passes to reach 1500 mPa s. At a DA of 35%, the viscosity reached a maximum value of 3400 mPa s after 1 pass and then decreased to 2500 mPa after 2 passes. At a DA of 22%, the maximum viscosity of 540 mPa s was observed after 1 pass, with decreases in viscosity observed with increasing passes.

As the DA decrease, fewer passes were required to decrease the NF width, as shown in Fig. 5–7. Thin NFs cause high viscosities because the number of entanglements between NFs increases as the number of NFs in water increases. However, as the number of passes increased, a decrease of the viscosity was observed at lower DAs, probably owing to a shortening of the NF length. It has been reported that the shortening of ChNFs by strong mechanical forces occurs with the Star Burst system when the number of passes exceeds 10 [25,26].

We obtained a maximum viscosity of 3400 mPa s after 1 pass at a DA of 35%. In our previous study [16], we observed a maximum viscosity of 2400–3700 mPa s for β-ChNFs at a DA of 95% under acidic conditions. The disintegration of β-chitin into NFs is easier than that of α-chitin because β-chitin does not have significant hydrogen bonding between the molecular sheets and can form a hydrate. In this work, following deacetylation of α-chitin, we obtained a NF dispersion with a high viscosity, similar to that of NF dispersions of β-chitin.

4. Discussion

As shown in Fig. 2b, a change in the deacetylation reaction rate was observed at a DA of approximately 70%. This change probably occurs because deacetylation proceeds

gradually from the surface to the interior of the ChNF bundle. Thus, the deacetylation is considered to proceed in two steps (1) on the surface of ChNF bundles and (2) in the interior of the ChNF bundles. Step (1) was completed quickly by a DA of approximately 70%, and then step (2) proceeded slowly, resulting in the observed change in the deacetylation reaction (Fig. 2b).

We propose a model for estimating the NF width at different DAs (Fig. 10). The average NF width at a DA of 95% after 10 passes was 34 nm (Fig. 5), and we used this width as the base cylindrical column at a DA of 100%. It was assumed that a decrease in DA corresponds to an increase in transformation of amide groups into amine groups and that the deacetylation process proceeds gradually from the surface to the interior of the NF column. Furthermore, we assumed that the deacetylated surface (white part) has a DA of 0% and the interior (black part) maintains a DA of 100%. Only the surface part could be dissolved after the acetic acid and Star Burst treatments and the interior part was isolated as the ChNFs after the disintegration process. If the whole cylindrical column was deacetylated completely, i.e., to chitosan, it would be dissolved by the acetic acid treatment, and not disintegrated to NFs.

At a DA of 66%, the average NF diameters were 28 nm (1 pass), 31 nm (2 passes), and 18 nm (10 passes) (Fig. 6). When deacetylation proceeded from the surface of the 34 nm column, a thickness of 3 nm from the surface was changed to amino groups. The dissolution of this part of the column by the acetic acid treatment would give a diameter of 28 nm (34 nm – 3 nm × 2), which is similar to the experimental values obtained after 1 and 2 passes. At this DA, as only the outermost surface was deacetylated, and, then dissolved by the acetic acid treatment, the NF diameter decreased gradually as the number of passes increased. As a result, the transmittance and the viscosity also increased gradually with the number of passes.

At a DA of 35%, the average NF diameters were 20 nm (1 pass), 19 nm (2 passes), and 18 nm (10 passes) (Fig. 7). If a thickness of 7 nm of the surface was dissolved by the

acetic acid and Star Burst treatments, the diameter would be evaluated as 20 nm (34 nm – 7 nm × 2), which is similar to the experimental values. As shown in Fig. 2b, the DA of 35% deacetylated chitin powder increased to 45% after the acid treatment, indicating that a thickness of 5.5 nm of the surface was dissolved by the acetic acid treatment, and the additional 1.5 nm was dissolved by the Star Burst treatment. At this DA, as almost all of the surface was deacetylated, the dissolution of the surface by the acetic acid treatment completely disrupted the contact between the cylindrical columns, resulting in a decrease of the NF diameter after only 1 pass. The surface of the cylindrical column changed from the deacetylated to the non-deacetylated unit; however, these ChNFs do not aggregate easily. Other research reported that non-deacetylated ChNFs (unmodified ChNFs) can be dispersed for a few months [3,16]. These results indicate that once the ChNFs are completely dispersed in water, they do not aggregate over the period of several months. In addition, if any deacetylated parts remained after the acid treatment, the amino groups would be protonated in the presence of acid. Thus, electrostatic repulsion between the NFs would increase, resulting in thin NFs with a narrow width distribution. As a result, the transmittance and the viscosity increased after only 1 pass. From this simple model of a cylindrical column, the NF diameter could be estimated using the DA.

5. Conclusions

The disintegration of α-chitin powder into NFs is more difficult than that of β-chitin because α-chitin has hydrogen bonds between the molecular chains. Therefore, the physicochemical properties, such as transmittance and viscosity, of α-ChNF dispersions are more difficult to control than those of β-ChNF dispersions. In this work, to weaken the hydrogen bonds between the α-chitin molecular chains, we used partial deacetylation of α-chitin. First, the α-chitin powder was deacetylated by alkaline treatment to obtain α-chitin

powders with varying DA. Then, the deacetylated part on the ChNF surface was dissolved by an acetic acid treatment. Subsequently, the solid residue was disintegrated into ChNFs using wet pulverization. As a result, we found that the average ChNF width decreased with decreasing DA. Furthermore, this decrease in the average ChNF width led to dispersions with higher transmittance and viscosity, similar to the values previously obtained for β-ChNF dispersions. In addition, we suggested a simple model for estimating the average ChNF width at different DAs and confirmed that the model agreed with the experimental results. These results indicate that the physicochemical properties of α-ChNFs can be controlled by changing the DA and that the DA can be used to estimate these properties. Recently, it has been reported that the chitosan NFs and the surface-deacetylated ChNFs promoted mouse hair growth [27]. The production of DA-controlled ChNFs will be important in medical applications.

Acknowledgments

Funding: This work was supported by JSPS KAKENHI [grant number 17H04893]. We thank Dr. Nobuhide Takahashi, Dr. Hiroshi Fukunaga, and Dr. Iori Shimada for their substantial intellectual contributions to project conception.

Competing interest

The authors declare no competing interests.

References

[1] N. Yan, X. Chen, Don't waste seafood waste. Turning cast-off shells into nitrogen-rich chemicals would benefit economies and the environment, Nature. 524 (2015) 155–157. https://doi.org/10.1038/524155a.

[2] D. Raabe, C. Sachs, P. Romano, The crustacean exoskeleton as an example of a structurally and mechanically graded biological nanocomposite material, Acta Mater. 53 (2005) 4281–4292. https://doi.org/10.1016/j.actamat.2005.05.027.

[3] S. Ifuku, H. Saimoto, Chitin nanofibers: Preparations, modifications, and applications, Nanoscale. 4 (2012) 3308–3318. https://doi.org/10.1039/c2nr30383c.

[4] I.F. Nata, S.S.S. Wang, T.M. Wu, C.K. Lee, β-Chitin nanofibrils for self-sustaining hydrogels preparation via hydrothermal treatment, Carbohydr. Polym. 90 (2012) 1509–1514. https://doi.org/10.1016/j.carbpol.2012.07.022.

[5] C. Chen, D. Li, Q. Hu, R. Wang, Properties of polymethyl methacrylate-based nanocomposites: Reinforced with ultra-long chitin nanofiber extracted from crab shells, Mater. Des. 56 (2014) 1049–1056. https://doi.org/10.1016/j.matdes.2013.11.057.

[6] S. Suenaga, M. Osada, Parameters of hydrothermal gelation of chitin nanofibers determined using a severity factor, Cellulose. 25 (2018) 6873–6885. https://doi.org/10.1007/s10570-018-2053-3.

[7] S. Suenaga, M. Osada, Preparation of β-chitin nanofiber aerogels by lyophilization, Int. J. Biol. Macromol. 126 (2019) 1145–1149. https://doi.org/10.1016/j.ijbiomac.2019.01.006.

[8] P. Sikorski, R. Hori, M. Wada, Revisit of α-chitin crystal structure using high resolution X-ray diffraction data, Biomacromolecules. 10 (2009) 1100–1105. https://doi.org/10.1021/bm801251e.

[9] F.C. Yang, R.D. Peters, H. Dies, M.C. Rheinstädter, Hierarchical, self-similar structure in native squid pen, Soft Matter. 10 (2014) 5541–5549. https://doi.org/10.1039/c4sm00301b.

[10] Y. Nishiyama, Y. Noishiki, M. Wada, X-ray structure of anhydrous β-chitin at 1 Å resolution, Macromolecules. 44 (2011) 950–957. https://doi.org/10.1021/ma102240r.

[11] D. Sawada, Y. Nishiyama, P. Langan, V.T. Forsyth, S. Kimura, M. Wada, Direct determination of the hydrogen bonding arrangement in anhydrous β-chitin by neutron fiber diffraction, Biomacromolecules. 13 (2012) 288–291. https://doi.org/10.1021/bm201512t.

[12] D. Sawada, Y. Nishiyama, P. Langan, V.T. Forsyth, S. Kimura, M. Wada, Water in crystalline fibers of dihydrate β-chitin results in unexpected absence of intramolecular hydrogen bonding, PLoS One. 7 (2012) 4–11. https://doi.org/10.1371/journal.pone.0039376.

[13] Y. Fan, T. Saito, A. Isogai, Preparation of chitin nanofibers from squid Pen β-chitin by simple mechanical treatment under acid conditions, Biomacromolecules. 9 (2008) 1919–1923. https://doi.org/10.1021/bm800178b.

[14] S. Suenaga, N. Nikaido, K. Totani, K. Kawasaki, Y. Ito, K. Yamashita, M. Osada, Effect of purification method of β-chitin from squid pen on the properties of β-chitin nanofibers, Int. J. Biol. Macromol. 91 (2016) 987–993. https://doi.org/10.1016/j.ijbiomac.2016.06.060.

[15] S. Ifuku, K. Yamada, M. Morimoto, H. Saimoto, Nanofibrillation of dry chitin powder by star burst system, J. Nanomater. 2012 (2012) 645624. https://doi.org/10.1155/2012/645624.

[16] S. Suenaga, K. Totani, Y. Nomura, K. Yamashita, I. Shimada, H. Fukunaga, N. Takahashi, M. Osada, Effect of acidity on the physicochemical properties of α- and β-

chitin nanofibers, Int. J. Biol. Macromol. 102 (2017) 358–366. https://doi.org/10.1016/j.ijbiomac.2017.04.011.

[17] S. Suenaga, M. Osada, Systematic dynamic viscoelasticity measurements for chitin nanofibers prepared with various concentrations, disintegration times, acidities, and crystalline structures, Int. J. Biol. Macromol. 115 (2018) 431–437. https://doi.org/10.1016/j.ijbiomac.2018.04.082.

[18] S. Ifuku, M. Nogi, K. Abe, M. Yoshioka, M. Morimoto, H. Saimoto, H. Yano, Preparation of chitin nanofibers with a uniform width as α-chitin from crab shells, Biomacromolecules. 10 (2009) 1584–1588. https://doi.org/10.1021/bm900163d.

[19] S. Ifuku, M. Nogi, M. Yoshioka, M. Morimoto, H. Yano, H. Saimoto, Fibrillation of dried chitin into 10-20 nm nanofibers by a simple grinding method under acidic conditions, Carbohydr. Polym. 81 (2010) 134–139. https://doi.org/10.1016/j.carbpol.2010.02.006.

[20] Y. Fan, T. Saito, A. Isogai, Individual chitin nano-whiskers prepared from partially deacetylated α-chitin by fibril surface cationization, Carbohydr. Polym. 79 (2010) 1046–1051. https://doi.org/10.1016/j.carbpol.2009.10.044.

[21] J. Brugnerotto, J. Lizardi, F.M. Goycoolea, W. Argüelles-Monal, J. Desbrières, M. Rinaudo, An infrared investigation in relation with chitin and chitosan characterization, Polymer. 42 (2001) 3569–3580. https://doi.org/10.1016/S0032-3861(00)00713-8.

[22] B.M. Min, S.W. Lee, J.N. Lim, Y. You, T.S. Lee, P.H. Kang, W.H. Park, Chitin and chitosan nanofibers: Electrospinning of chitin and deacetylation of chitin nanofibers, Polymer. 45 (2004) 7137–7142. https://doi.org/10.1016/j.polymer.2004.08.048.

[23] J. Xu, L. Liu, J. Yu, Y. Zou, Z. Wang, Y. Fan, DDA (degree of deacetylation) and pH-dependent antibacterial properties of chitin nanofibers against Escherichia coli,

Cellulose. 26 (2019) 2279–2290. https://doi.org/10.1007/s10570-019-02287-2.

[24] R. Kose, T. Kondo, Favorable 3D-network formation of chitin nanofibers dispersed in water prepared using aqueous counter collision, Sen'i Gakkaishi. 67 (2011) 91–95. https://doi.org/10.2115/fiber.67.91.

[25] A.K. Dutta, N. Kawamoto, G. Sugino, H. Izawa, M. Morimoto, H. Saimoto, S. Ifuku, Simple preparation of chitosan nanofibers from dry chitosan powder by the star burst system, Carbohydr. Polym. 97 (2013) 363–367. https://doi.org/10.1016/j.carbpol.2013.05.010.

[26] A.K. Dutta, H. Izawa, M. Morimoto, H. Saimoto, S. Ifuku, Simple preparation of chitin nanofibers from dry squid pen β-chitin powder by the star burst system, J. Chitin Chitosan Sci. 1 (2014) 186–191. https://doi.org/10.1166/jcc.2013.1023.

[27] K. Azuma, R. Koizumi, H. Izawa, M. Morimoto, H. Saimoto, T. Osaki, N. Ito, M. Yamashita, T. Tsuka, T. Imagawa, Y. Okamoto, T. Inoue, S. Ifuku, Hair growth-promoting activities of chitosan and surface-deacetylated chitin nanofibers, Int. J. Biol. Macromol. 126 (2019) 11–17. https://doi.org/10.1016/j.ijbiomac.2018.12.135.

Figure captions

Fig. 1. Preparation of deacetylated α-ChNFs.

Fig. 2. Effect of NaOH aqueous solution treatment time on DA. (b) Magnified illustration of (a). Deacetylated chitin powder (○), solid residue (□) shown in Fig. 1.

Fig. 3. Effect of DA on the weight change of α-chitin.

Fig. 4. FT-IR spectra of deacetylated chitin powder with different DAs.

Fig. 5. FE-SEM image and width distribution of α-ChNFs at DA = 95%.

Fig. 6. FE-SEM images and width distributions of α-ChNFs at DA = 66%.

Fig. 7. FE-SEM images and width distributions of α-ChNFs at DA = 35%.

Fig. 8. Effect of DA on the transmittance and photographs of α-ChNF dispersions.

Fig. 9. Effect of DA on the viscosity of α-ChNF dispersions.

Fig. 10. Model for estimating NF width at different DAs.

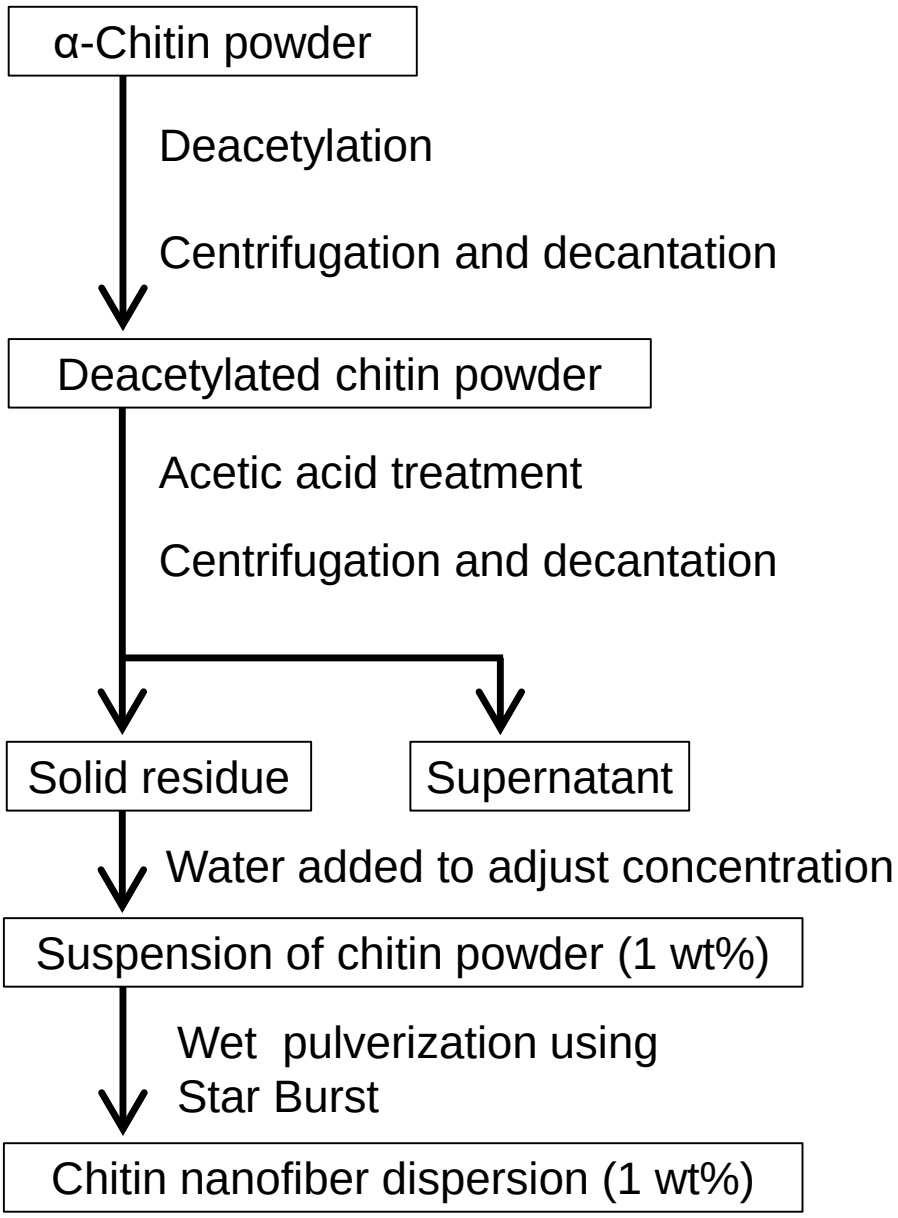

J. Machida et al. Fig. 1

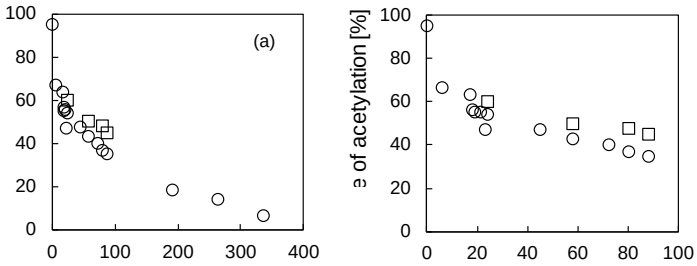

J. Machida et al. Fig. 2

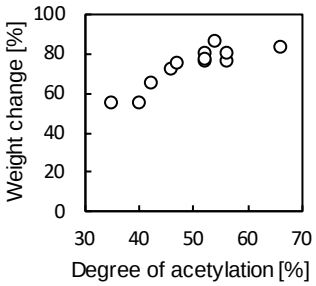

J. Machida et al. Fig. 3

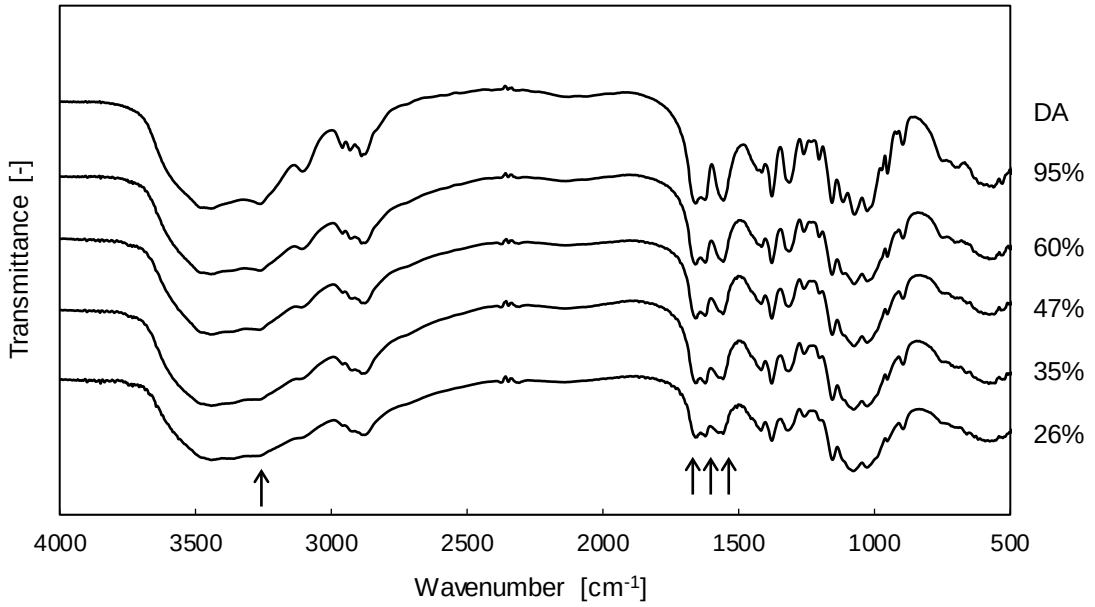

J. Machida et al. Fig. 4

445

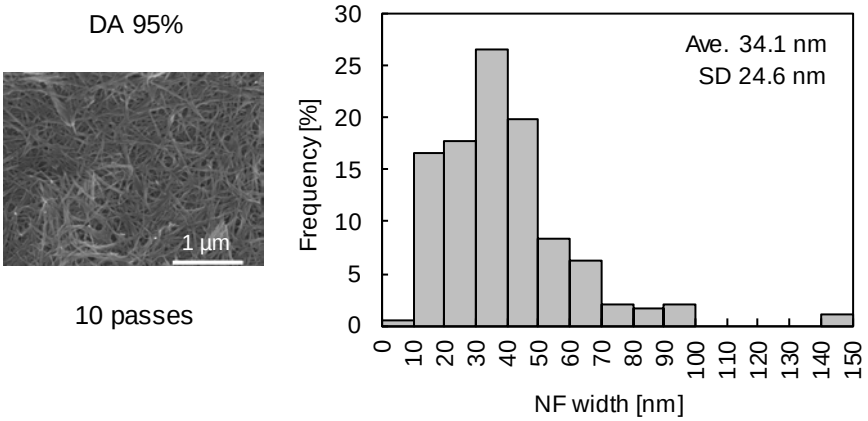

446
447
448
449
450 J. Machida et al. Fig. 5
451

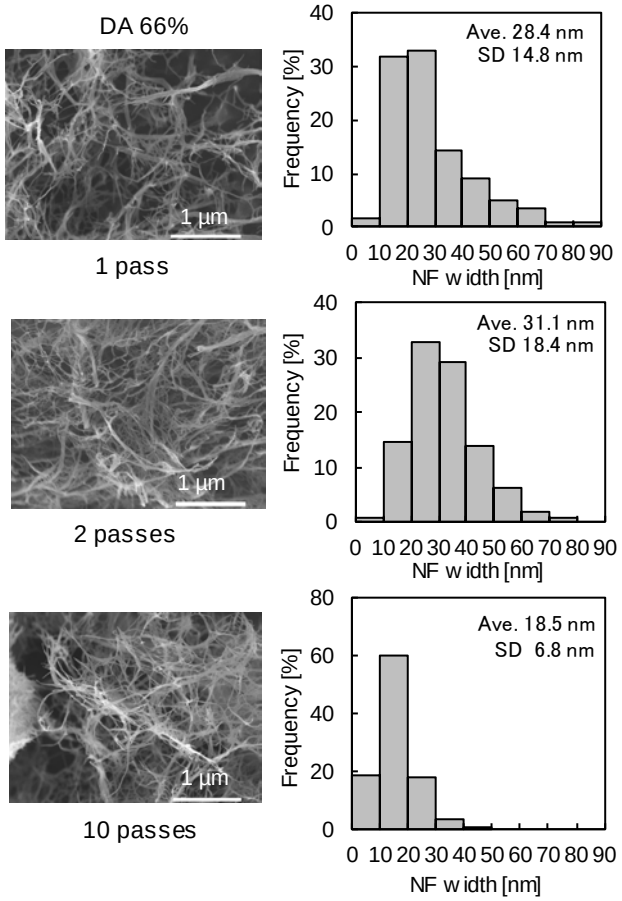

J. Machida et al. Fig. 6

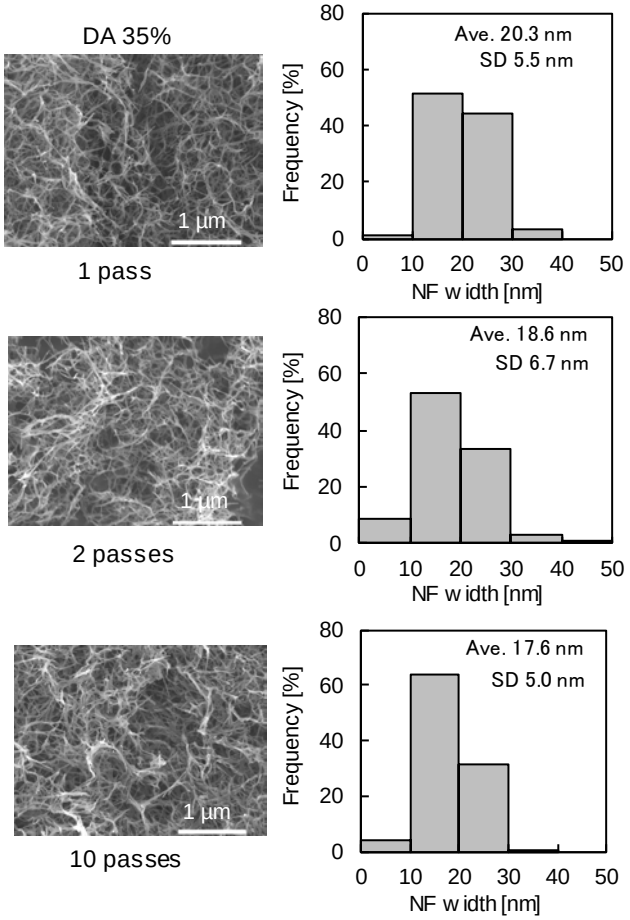

J. Machida et al. Fig. 7

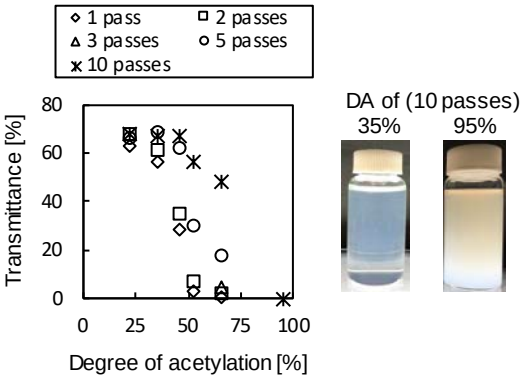

J. Machida et al. Fig. 8

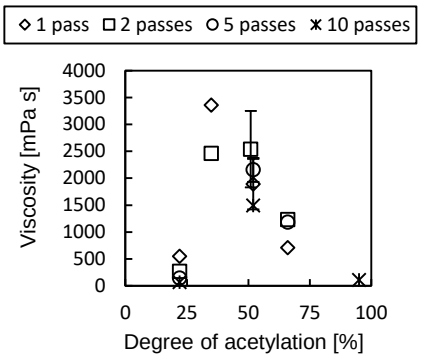

J. Machida et al. Fig. 9

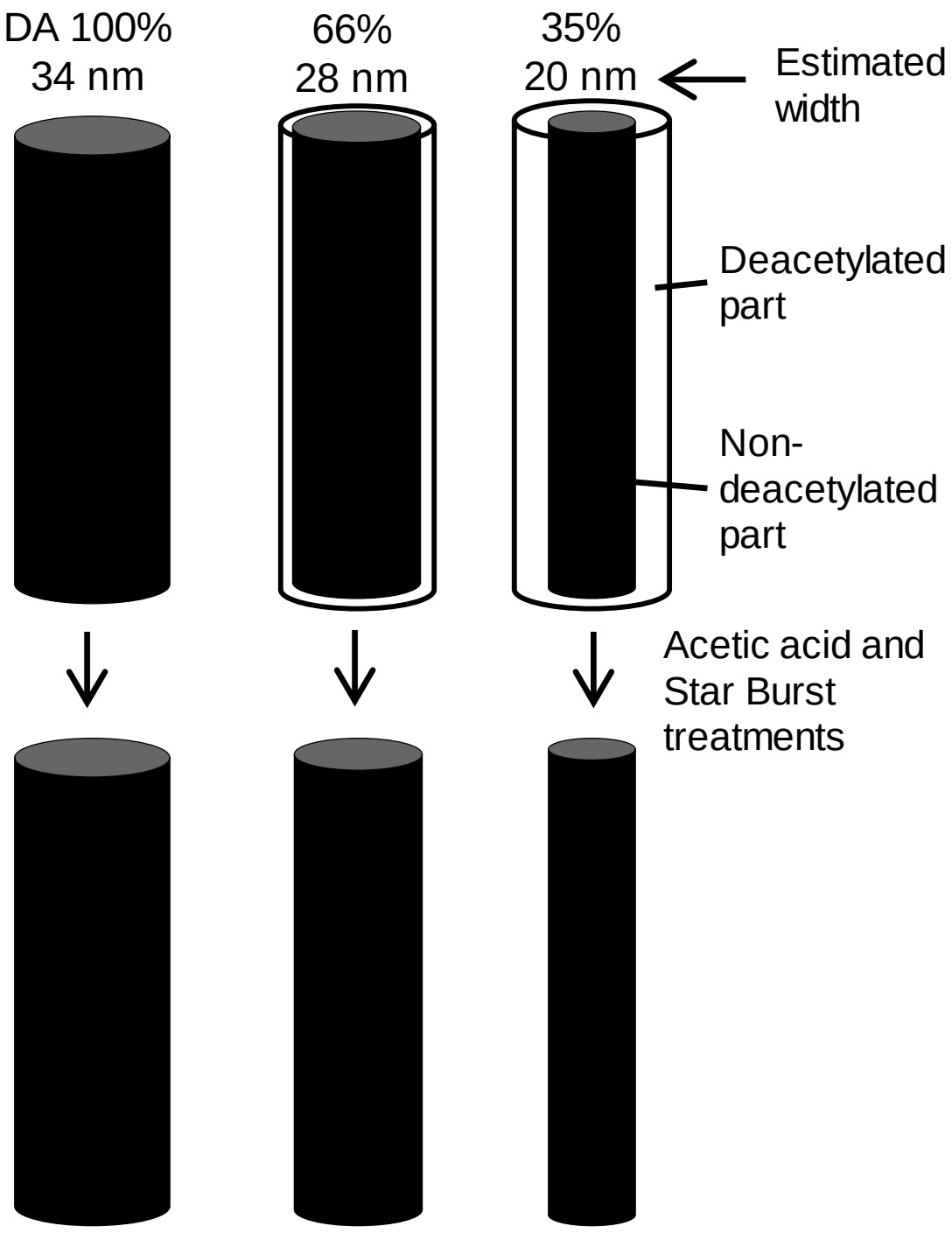

J. Machida et al. Fig. 10